JCTA Journal of Computing Theories and Applications ISSN:3024-9104

Research Article

Effectiveness and Limitations of Preprocessing Methods for Proprioceptive Sensor Noise in Quadruped Robots

Mui D. Nguyen [1], Minh T. Nguyen [1,*], Ha T. Nguyen [2], Binh TT. Nguyen [2], Long Q. Dinh [3], Dung T. Nguyen [3], Thang C. Vu [3], and Duc M. Ngo [1]

[1] Thai Nguyen University of Technology, Thai Nguyen University, Thai Nguyen 24000, Viet Nam; e-mail : ducmui@tnut.edu.vn, nguyentuanminh@tnut.edu.vn; ngoduc198-tdh@tnut.edu.vn
[2] Thai Nguyen University, Thai Nguyen 24000, Viet Nam; e-mail : hant@tnu.edu.vn; binhntt@tnu.edu.vn
[3] Thai Nguyen University of Information and Communication Technology, Thai Nguyen 24000, Viet Nam; e-mail : vcthang@ictu.edu.vn; ntdungcndt@ictu.edu.vn; dqlong@ictu.edu.vn
***** Corresponding Author : Minh T. Nguyen

Abstract: Proprioceptive sensor data, including inertial measurement units (IMU), joint encoders, and torque sensors, plays a critical role in state estimation for quadruped robots operating in dynamic and unstructured environments. However, these signals are often degraded by various sources of error, such as high-frequency noise, bias, drift, and contact-induced disturbances, which directly affect estimation accuracy and stability. This study presents a systematic analysis of sensor-specific noise characteristics and evaluates the effectiveness of preprocessing methods tailored to each sensor modality. Specifically, moving average filtering is applied to encoder signals to mitigate noise amplification during differentiation, while first-order low-pass filtering is employed for IMU and torque signals to suppress high-frequency noise. Experimental results on a publicly available quadruped dataset demonstrate that encoder velocity RMSE is reduced by 12.09%, high-frequency energy decreases by 59.63%, and signal-to-noise ratio (SNR) improves by 145.6%. However, variance reductions remain limited (3.39% for IMU and 4.05% for torque), indicating the persistence of impulsive, non-Gaussian noise caused by contact events. These findings highlight that linear preprocessing methods are effective for attenuating high-frequency noise but insufficient for handling non-Gaussian disturbances. The study provides practical insights into the effectiveness and limitations of preprocessing strategies, serving as a foundation for developing more robust signal processing and state estimation frameworks in quadruped robotics.

Keywords: Encoder signal processing; IMU noise analysis; Quadruped robots; Sensor data preprocessing; Signal-to-noise ratio; State estimation; Sustainable robotics; Torque sensor analysis.

Received: March, 23rd 2026
Revised: April, 21st 2026
Accepted: April, 24th 2026
Published: April, 28th 2026

Copyright: © 2026 by the authors. Submitted for possible open access publication under the terms and conditions of the Creative Commons Attribution (CC BY) licenses (https://creativecommons.org/licenses/by/4.0/)

1. Introduction

Quadruped robots have gained increasing attention due to their ability to traverse complex, unstructured, and obstacle-rich terrains, often outperforming wheeled or tracked platforms in challenging environments [1], [2]. Their applications span a wide range of domains, including industrial inspection, exploration, disaster response, and logistics in uncertain and dynamic conditions [3]–[5]. To ensure stable and reliable locomotion, accurate state estimation is essential, as it provides critical information regarding body motion, joint states, and interactions with the environment [6]–[9]. Sensor systems in quadruped robots can generally be categorized into proprioceptive and exteroceptive sensors, as illustrated in Figure 1. Proprioceptive sensors—such as inertial measurement units (IMUs), joint encoders, and torque sensors—provide direct measurements of the robot's internal kinematic and dynamic states. In contrast, exteroceptive sensors, including cameras, LiDAR, and radar, provide information about the surrounding environment and external context.

However, in many dynamic motion scenarios and complex environments, exteroceptive sensor data may become unreliable, intermittent, or unavailable. As a result, state estimation systems in quadruped robots often rely heavily on proprioceptive sensing [10]–[12]. To

improve estimation accuracy and robustness, various advanced approaches—such as the Extended Kalman Filter (EKF), Invariant EKF (InEKF), and graph-based methods—have been developed to fuse multi-sensor information under nonlinear system dynamics [13]–[16]. These estimation frameworks are inherently probabilistic, where measurement noise directly affects the innovation term and covariance update, making them highly sensitive to the quality of input sensor data [17].

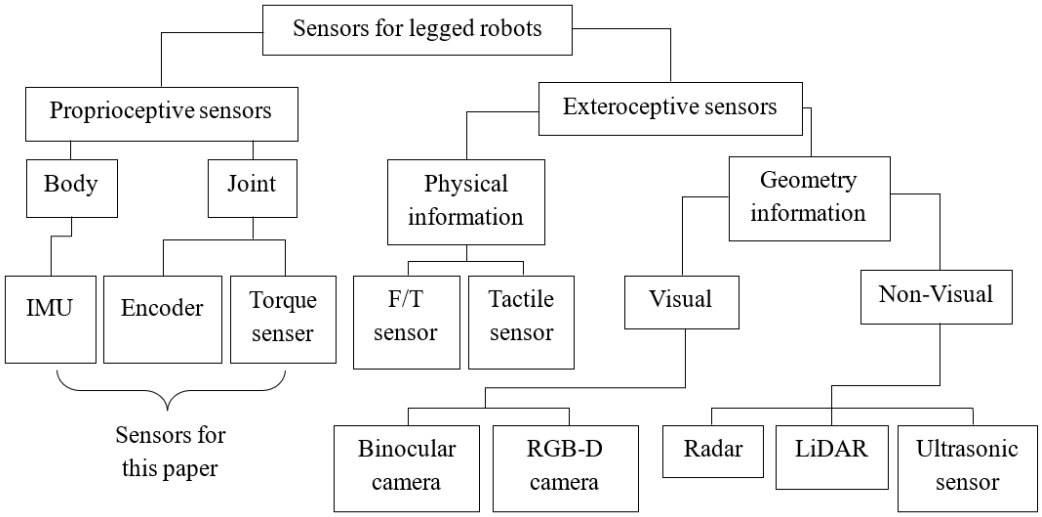

Figure 1. Proprioceptive and exteroceptive sensor taxonomy for legged robots [18].

In practice, proprioceptive sensor measurements are affected by multiple sources of error, including noise, bias, quantization, time synchronization issues, and contact-induced disturbances [19]–[21]. Intermittent foot–ground contact generates high-frequency impulses and oscillations, significantly altering signal characteristics. Specifically, IMU measurements are subject to drift; encoder signals suffer from noise amplification during numerical differentiation; and torque signals exhibit spike-like disturbances during contact events [22]. Despite significant advances in state estimation algorithms, most existing studies focus primarily on improving estimation frameworks, while the quality and characteristics of raw proprioceptive sensor data are often overlooked. In particular, there is a lack of systematic analysis of how different types of sensor noise—such as high-frequency noise, bias, drift, and contact-induced disturbances—affect preprocessing and, consequently, influence estimation performance. This limitation is particularly critical in quadruped robots operating in dynamic environments, where intermittent contact events introduce impulsive and non-Gaussian noise. Since estimation performance is fundamentally constrained by the quality of input measurements, a detailed analysis of preprocessing methods is essential for ensuring reliable state estimation.

Motivated by this gap, this paper presents a systematic analysis of proprioceptive sensor signal characteristics and evaluates sensor-specific preprocessing methods in quadruped robots. Rather than proposing a new state estimation algorithm, this study focuses on signal-level challenges that directly impact estimation performance. The main contributions of this work are summarized as follows:

- A systematic analysis of noise characteristics in proprioceptive sensors (IMU, encoder, and torque) in quadruped robots;
- An experimental evaluation of sensor-specific preprocessing methods and their effectiveness;
- Insights into the limitations of linear filtering methods when handling non-Gaussian and contact-induced noise.

From a state estimation perspective, the quality of sensor measurements directly influences the performance of estimators such as EKF and InEKF. Measurement noise affects both the innovation term and covariance update, thereby impacting estimation accuracy and stability. Therefore, improving sensor data quality through appropriate preprocessing is a critical step toward achieving reliable and robust state estimation in quadruped robots. The remainder of this paper is organized as follows. Section 2 describes the characteristics and error

sources of proprioceptive sensor signals. Section 3 presents the proposed preprocessing pipeline. Section 4 provides experimental results and quantitative evaluation. Finally, Section 5 concludes the paper..

2. Characteristics of Proprioceptive Sensor Signals

2.1. Inertial Measurement Unit (IMU)

The IMU provides information about the robot's body motion by measuring linear acceleration and angular velocity at high sampling rates. In quadruped robots, this sensor serves as a primary source for estimating short-term body orientation and kinematics, particularly when exteroceptive sensing is unreliable or unavailable. The IMU is typically mounted near the robot's center of mass, as illustrated in Figure 2. This placement minimizes the influence of limb-induced vibrations and reduces disturbances caused by ground contact. In addition, the IMU reference frame is commonly assumed to coincide with the robot body frame, which simplifies state estimation models, particularly in Kalman filter-based approaches such as EKF and InEKF [23], [24].

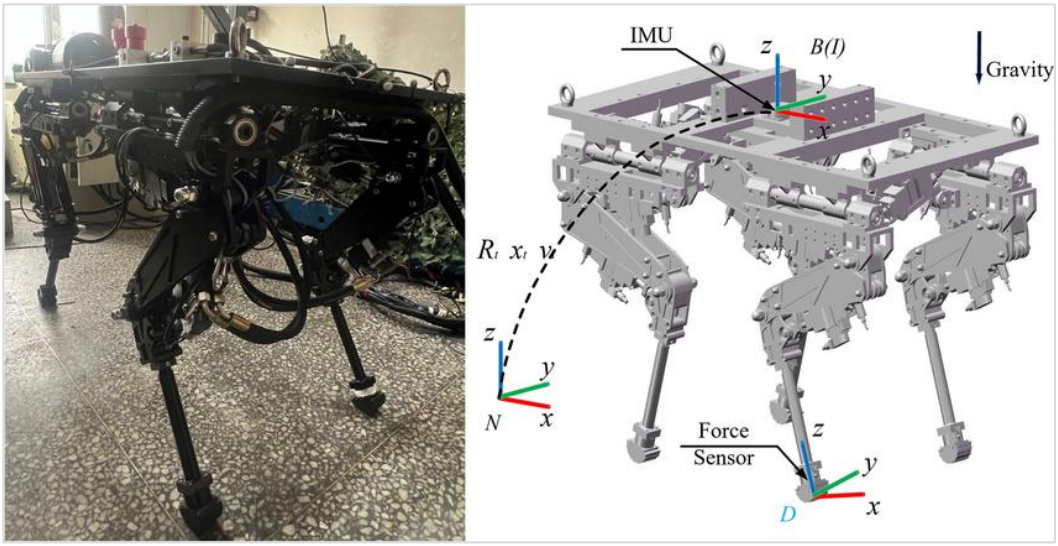

Figure 2. IMU placement in a quadruped robot body [25].

Despite its importance, IMU measurements are significantly affected by mechanical vibrations and impact forces during locomotion. These disturbances introduce measurement noise and lead to cumulative errors over time. Consequently, raw IMU data cannot be directly used and must be preprocessed before being integrated into state estimation algorithms. The bias and drift characteristics of the IMU can be modeled as follows. The measured angular velocity signal is expressed as:

$$\omega_m(k) = \omega(k) + b + n(k) \tag{1}$$

where b represents the bias and $n(k)$ denotes measurement noise. In practice, the bias is estimated during a stationary phase:
In practice, the bias is estimated during a stationary phase:

$$\hat{b} = \frac{1}{N}\sum_{k=1}^{N} \omega_m\,(k) \tag{2}$$

After bias removal, the corrected signal becomes:

$$\omega_c(k) = \omega_m(k) - \hat{b} \tag{3}$$

To model drift over time, the bias is represented as a random walk process:

$$b_{rw}(k) = b_{rw}(k-1) + \sigma w_k \tag{4}$$

where w_k is Gaussian noise.
The resulting drift-affected signal is given by:

$$\omega_d(k) = \omega_c(k) + b_{rw}(k) \tag{5}$$

This formulation captures the drift behavior commonly observed in IMU signals, especially under sustained vibration and repeated impact conditions.

2.2. Encoder Sensors

Joint encoders are intrinsic sensors used to measure joint angles in real time. In quadruped robots, they are typically installed at the hip, thigh, and knee joints, as shown in Figure 3, providing essential input for kinematic modeling and state estimation [26].

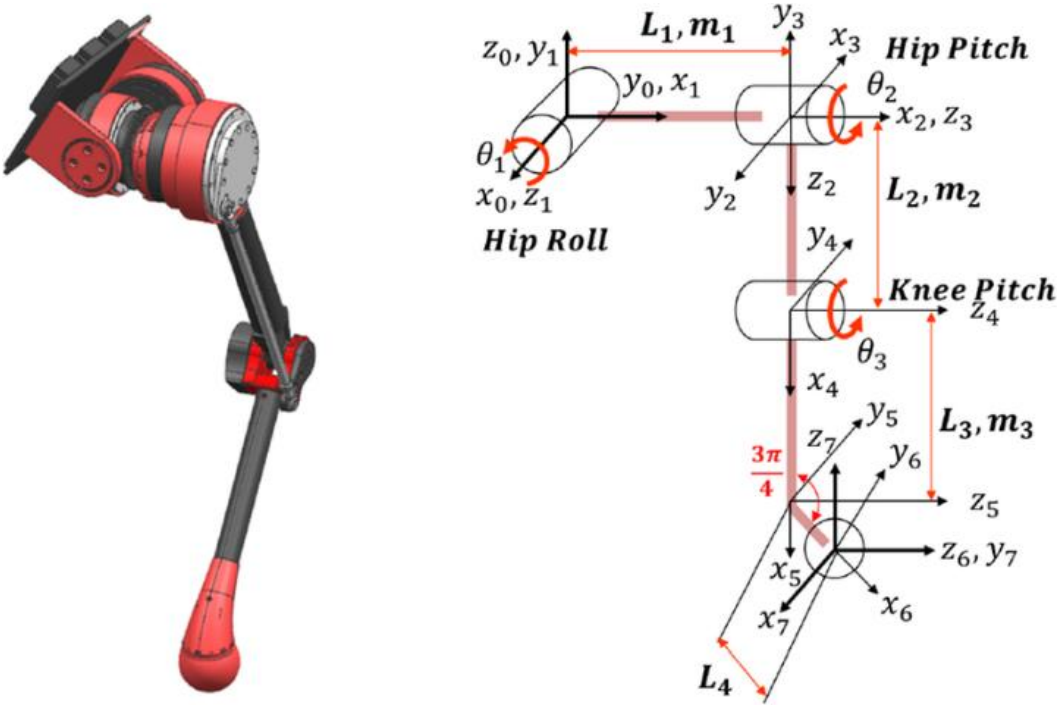

Figure 3. Joint encoder placement in a quadruped robot leg [27].

However, encoder measurements are inherently relative and do not directly provide absolute motion information. In practice, joint velocity is often computed via numerical differentiation of position signals, which significantly amplifies noise and quantization errors, particularly during rapid movements or contact events.

The effect of numerical differentiation on noise amplification is expressed as follows. Let $q(t)$ denote the joint angle signal, and the joint velocity is computed using a central difference approximation:

$$\dot{q}(k) = \frac{q(k+1) - q(k-1)}{2\Delta t} \tag{6}$$

This operation amplifies high-frequency noise components in $q(k)$, leading to:

$$\dot{q}(k) = \dot{q}_{true}(k) + \epsilon(k) \tag{7}$$

where $\epsilon(k)$ represents noise amplification in the high-frequency domain.

Experimental observations indicate that velocity signals derived through numerical differentiation exhibit significantly higher noise levels compared to directly measured signals, especially during dynamic motion phases.

2.3. Joint Torque Sensors

Joint torque sensors measure interaction forces between the robot and its environment and are commonly used to detect contact states in quadruped locomotion. Variations in torque signals reflect transitions between stance and swing phases, providing valuable information for control and estimation.

However, torque measurements are highly sensitive to contact events. Foot–ground interactions generate impulsive disturbances, resulting in spikes and high-frequency noise components. These disturbances are inherently non-Gaussian and cannot be effectively mitigated using simple linear filtering techniques.

Contact-induced disturbances in torque signals are modeled as follows. The measured torque signal is expressed as:

$$\tau_m(k) = \tau(k) + d_c(k) \tag{8}$$

where $d_c(k)$ represents contact-induced noise.

In practice, $d_c(k)$ appears as large-amplitude, discontinuous spikes in the signal. These disturbances exhibit impulsive behavior and deviate significantly from Gaussian distributions, making them difficult to suppress using conventional linear filters. Therefore, preprocessing of torque signals must be performed carefully to reduce noise while preserving meaningful information related to contact dynamics, which is essential for reliable state estimation and control.

3. Sensor Data Preprocessing

The overall preprocessing workflow adopted in this study is illustrated in Figure 4. This pipeline summarizes the sequence of processing steps applied to each sensor type, starting from raw data acquisition, followed by noise characteristic analysis, sensor-specific preprocessing, normalization, and subsequent evaluation.

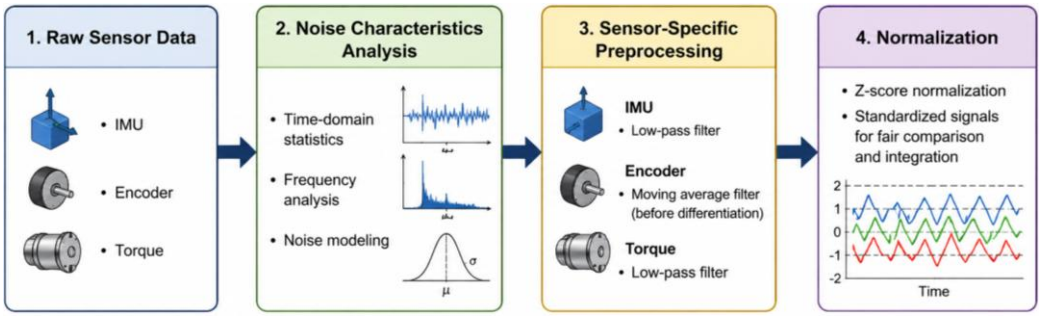

Figure 4. Preprocessing pipeline for proprioceptive sensor data in quadruped robots.

Proprioceptive sensor data in quadruped robots exhibits distinct noise characteristics depending on the sensor modality. Consequently, a single preprocessing method is not sufficient for all sensor types. Encoder signals are primarily affected by noise amplification due to numerical differentiation; IMU signals are dominated by high-frequency noise and cumulative bias; while torque signals contain impulsive disturbances caused by contact events. Therefore, preprocessing methods are selected based on the specific characteristics of each signal. The primary objective is to reduce noise while preserving essential dynamic information required for reliable state estimation.

3.1. Moving Average Filter for Encoders

Encoder signals provide joint position measurements, while joint velocity is typically obtained through numerical differentiation. This operation amplifies high-frequency noise, resulting in significant errors in the velocity signal. To mitigate this issue, the position signal is first smoothed using a moving average filter before differentiation. The filtered position signal is expressed as:

$$\tilde{q}(k) = \frac{1}{M}\sum_{i=0}^{M-1} q(k-i) \tag{9}$$

where M is the window size.

In this study, a window size of 10 samples is employed. This value is empirically selected to balance noise reduction and preservation of dynamic characteristics. The joint velocity is then computed from the filtered signal using:

$$\dot{q}_f(k) = \frac{\tilde{q}(k+1) - \tilde{q}(k-1)}{2\Delta t} \tag{10}$$

This approach reduces noise prior to differentiation, thereby limiting noise amplification while maintaining the overall dynamic behavior of the system.

3.2. Low-Pass Filtering for IMU and Torque Sensors

Both IMU and torque signals contain significant high-frequency noise components resulting from mechanical vibrations and contact events. In addition, torque signals are affected by impulsive disturbances that are distributed across a wide frequency range. To attenuate high-frequency noise, a first-order low-pass filter is applied:

$$y(k) = \alpha x(k) + (1-\alpha)y(k-1) \tag{11}$$

where $0 < \alpha < 1$ is the filter coefficient.

This recursive filter reduces noise while preserving signal continuity. However, smaller values of α result in increased smoothing at the cost of signal delay, which may degrade fast dynamic responses. In this work, α=0.2 is selected based on empirical tuning to achieve a balance between noise attenuation and temporal responsiveness.

While the low-pass filter effectively reduces high-frequency noise in IMU signals, its effectiveness is limited for torque signals due to the presence of non-Gaussian, impulsive disturbances caused by contact. As a result, only partial noise suppression can be achieved for torque measurements using this approach.

3.3. Data Normalization

To ensure consistent scaling across different sensor modalities, data normalization is applied. In this study, Z-score normalization is adopted due to its simplicity and effectiveness in handling multi-sensor data with different units and magnitudes. The normalized signal is defined as:

$$x_{norm} = \frac{x-\mu}{\sigma} \tag{11}$$

where μ and σ denote the mean and standard deviation of the signal, respectively.

It is important to emphasize that normalization does not directly reduce noise. Instead, it standardizes the data scale, facilitating comparison across sensors, improving numerical stability, and supporting multi-sensor integration.

3.4. Implications for State Estimation

The effectiveness of preprocessing extends beyond signal-level improvements and has direct implications for state estimation. In Kalman filter-based frameworks such as EKF and InEKF, measurement noise characteristics determine the reliability of sensor updates. Reducing high-frequency noise improves measurement consistency and can lead to reduced estimation variance and more stable state estimates. However, non-Gaussian disturbances—such as impulsive noise in torque signals caused by contact events—cannot be adequately modeled under standard Gaussian assumptions. This mismatch may degrade estimator performance and highlights the need for more advanced preprocessing or robust estimation techniques.

In typical EKF/InEKF frameworks, the state is updated using sensor measurements and their associated noise models. Therefore, improving the statistical properties of sensor data through preprocessing can lead to more consistent innovation updates and reduced estimation uncertainty. It should be noted that the implementation of a complete state

estimation algorithm is beyond the scope of this study. Instead, this work focuses on signal-level preprocessing as a fundamental step that supports downstream estimation methods.

Table 1. This is a table. Tables should be placed in the main text near to the first time they are cited.

Method	Sensor	Parameter	Value
Moving Average Filter	Encoder	Window size (M)	10 samples
Low-pass Filter	IMU	Coefficient (α)	0.2 (first-order)
Low-pass Filter	Torque	Coefficient (α)	0.2 (first-order)
Normalization	All	Method	Z-score

The parameters listed in Table 1 are empirically selected to balance noise reduction and preservation of dynamic characteristics. In particular, the moving average window size mitigates noise amplification during differentiation, while the low-pass filter coefficient controls the trade-off between smoothing and signal delay. All parameters are fixed across experiments to ensure consistency and reproducibility.

4. Experimental Results and Discussion

4.1. Experimental Setup

The experimental analysis follows the preprocessing pipeline illustrated in Figure 4. The experiments are conducted using the Proprioceptive Sensor Dataset for Quadruped Robots available on IEEE Dataport [28]. The dataset contains synchronized measurements from IMU, joint encoders, and torque sensors, with a duration of approximately 350 seconds and a sampling frequency of approximately 400 Hz.

The analysis focuses on evaluating the effects of noise, bias, and preprocessing methods on IMU, encoder, and torque signals. All results are obtained from a single dataset sequence without averaging across multiple trials. The dataset provides continuous and synchronized measurements, enabling consistent evaluation of preprocessing performance under identical motion conditions.

4.2. Effect of Moving Average Filtering on Encoder Signals

Figure 5 illustrates the effect of applying a moving average filter to encoder signals.

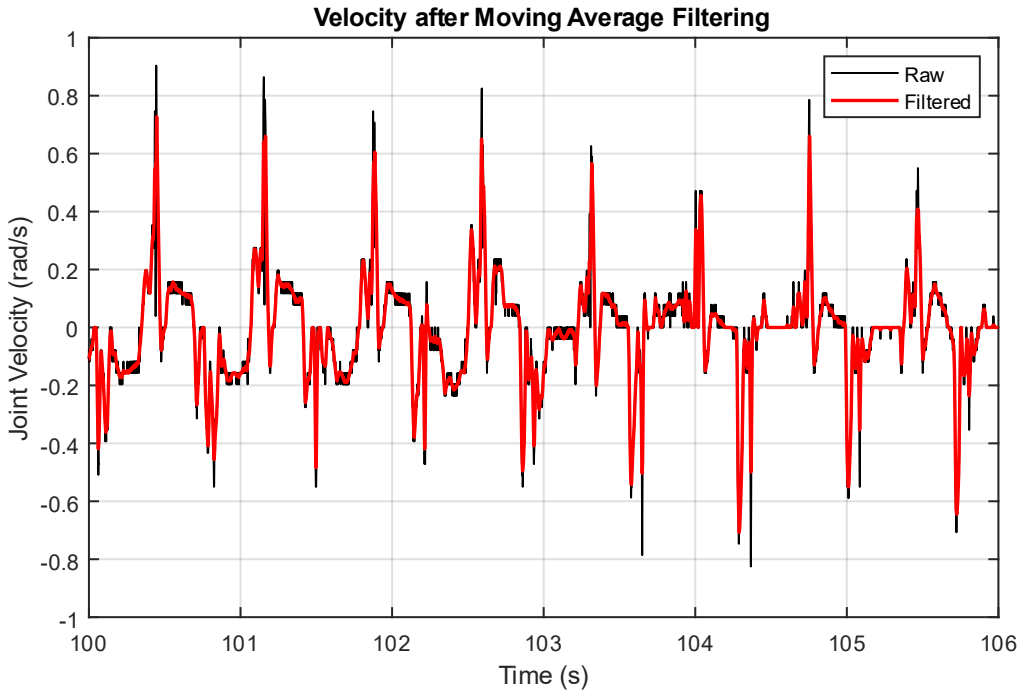

Figure 5. Comparison of encoder signals before and after applying a moving average filter.

Since the original position signal is relatively smooth, the difference between raw and filtered signals is not significant at the position level. However, when considering the velocity signal obtained through numerical differentiation, the improvement becomes substantial. The velocity derived from raw encoder data exhibits significant noise due to amplification during differentiation. After applying the moving average filter prior to differentiation, the noise level is significantly reduced, resulting in a smoother and more stable velocity profile. This confirms that pre-smoothing is essential for mitigating noise amplification and improving the quality of velocity estimation.

4.3. Effect of Low-Pass Filtering on IMU and Torque Signals

The effect of low-pass filtering on IMU and torque signals is presented in Figure 6. For IMU signals, the low-pass filter effectively suppresses high-frequency noise caused by mechanical vibrations while preserving the overall signal trend. This improves the stability of integrated quantities, such as orientation estimates. For torque signals, the filtering process exhibits more complex behavior. While the signal-to-noise ratio (SNR) increases significantly (145.6%) and high-frequency energy decreases by 59.63%, the variance shows only a minor reduction (4.05%). This discrepancy is attributed to impulsive, non-Gaussian noise caused by foot–ground contact. Although the filter attenuates high-frequency components, it cannot fully suppress large-amplitude spikes, which continue to dominate the variance. Furthermore, low-pass filtering only partially reduces contact-induced disturbances and may also attenuate meaningful contact-related information. This highlights a trade-off between noise reduction and preservation of physically relevant signal characteristics.

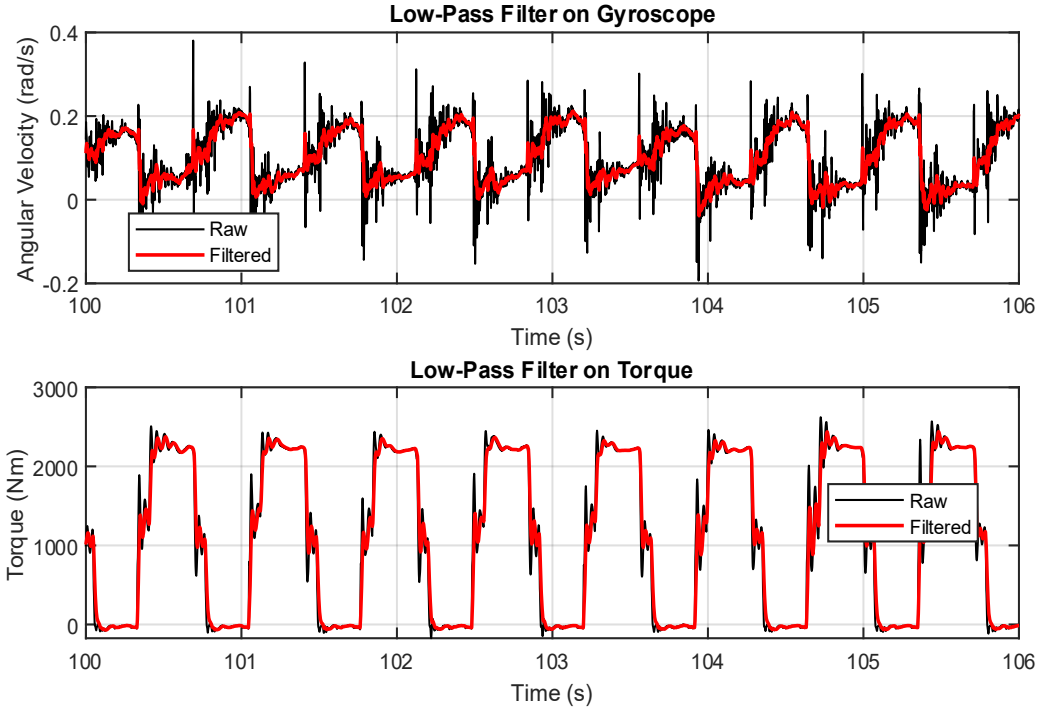

Figure 6. Results of applying a low-pass filter to IMU and torque signals.

4.4. Effect of Data Normalization

The effect of normalization on multi-sensor signals is shown in Figure 7. Normalization brings all sensor signals to a common scale, facilitating comparison and integration across different modalities. It does not alter noise characteristics or reduce signal variance but standardizes the magnitude of the signals. This transformation is particularly beneficial in multi-sensor fusion and learning-based frameworks, where differences in signal magnitude may bias the processing. By ensuring consistent scaling, normalization improves numerical stability and enables balanced contributions from IMU, encoder, and torque signals.

4.5. Evaluation Metrics and Quantitative Results

The evaluation employs multiple metrics to capture different aspects of signal quality. RMSE is used to quantify the error in encoder-derived velocity signals. Variance measures overall signal dispersion, while SNR evaluates signal quality as the ratio of signal power to noise power. High-frequency energy is computed using Fast Fourier Transform (FFT) to capture frequency-domain noise characteristics. It is important to note that variance alone is insufficient to characterize impulsive and non-Gaussian noise. Therefore, additional statistical measures are considered. Kurtosis is used to quantify heavy-tailed distributions caused by spike-like disturbances, while power spectral density (PSD) analysis provides a more detailed frequency-domain representation. These measures complement variance-based evaluation; however, a full quantitative analysis using these metrics is left for future work.

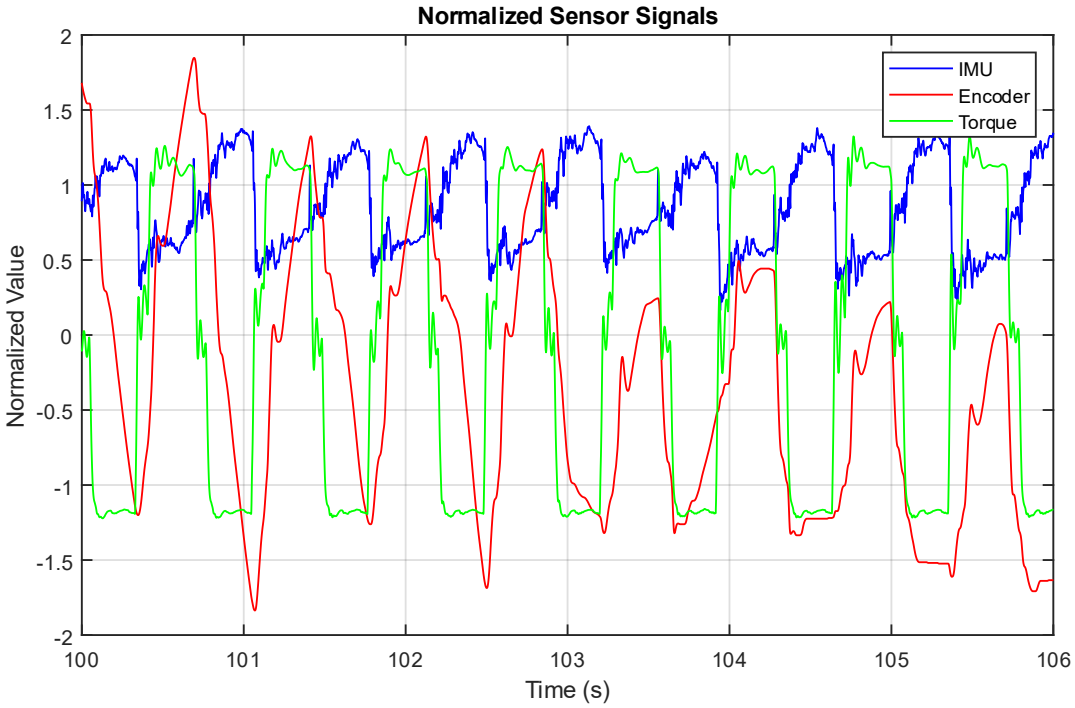

Figure 7. Normalized sensor signals after preprocessing.

Table 2. Quantitative evaluation of preprocessing methods on IMU, encoder, and torque signals.

Sensors	Metric	Raw	Filtered	Improvement
Torque	High-frequency energy	3.0644×10^{15}	1.2370×10^{15}	↓ 59.63%
	Signal-to-noise ratio	18.896	46.396	↑ 145.6%
	Variance	1.0102×10^{6}	9.6919×10^{5}	↓ 4.05%
Encoder	RMSE	0.0387	0.0340	↓ 12.09%
IMU	Variance	0.0430	0.0415	↓ 3.39%

The selection of evaluation metrics is aligned with the characteristics of each sensor. For encoder signals, RMSE captures the error introduced by differentiation and reflects the effectiveness of preprocessing in reducing this error. For IMU signals, variance and high-frequency energy quantify noise reduction, particularly for vibration-induced disturbances. For torque signals, a combination of SNR, variance, and high-frequency energy is used to evaluate performance under non-Gaussian noise conditions.

4.6. Discussion

The results demonstrate that the effectiveness of preprocessing methods strongly depends on the noise characteristics of each sensor. For encoder signals, moving average filtering reduces noise amplification during differentiation, leading to a clear improvement in RMSE (12.09%). For IMU signals, low-pass filtering effectively reduces high-frequency noise,

as reflected by a significant decrease in high-frequency energy, while maintaining the signal's dynamic trend. For torque signals, the results reveal a more complex behavior. The significant increase in SNR, combined with a small reduction in variance, indicates the presence of impulsive, non-Gaussian noise caused by contact events. These spike-like disturbances are not fully attenuated by linear filters and continue to dominate the variance. This highlights a fundamental limitation of linear preprocessing methods in handling contact-induced noise.

Additionally, robot motion conditions—particularly dynamic contact interactions—introduce both high-frequency and impulsive disturbances, which affect preprocessing performance differently across sensors. This further emphasizes the need for sensor-specific preprocessing strategies. From a state estimation perspective, improved signal quality contributes to more stable estimation performance in EKF and InEKF frameworks. Reduced high-frequency noise leads to more consistent measurements and improved integration stability. However, the persistence of impulsive noise suggests that conventional linear filtering is insufficient for robust estimation in real-world conditions.

4.7. Limitations and Future Work

Despite the observed improvements, several limitations remain. The limited reduction in variance for torque signals indicates that linear filters are not effective for suppressing impulsive, non-Gaussian disturbances caused by contact dynamics. This suggests the need for more advanced preprocessing approaches, such as nonlinear or robust filtering techniques. Future work should also integrate preprocessing with state estimation frameworks (e.g., EKF/InEKF) to quantitatively evaluate its impact on estimation accuracy. In addition, further studies should investigate the influence of different locomotion modes and dynamic conditions on preprocessing performance.

5. Conclusions

This paper presents a systematic analysis of proprioceptive sensor signal characteristics and sensor-specific preprocessing methods for quadruped robots. The study demonstrates that preprocessing effectiveness strongly depends on the underlying noise characteristics of each sensor modality. In particular, moving average filtering effectively reduces noise amplification in encoder-derived velocity, while low-pass filtering significantly attenuates high-frequency noise in IMU signals. For torque signals, although improvements in signal quality are observed—such as increased SNR and reduced high-frequency energy—impulsive, contact-induced disturbances remain largely unaffected.

These findings confirm that linear preprocessing methods are effective for handling Gaussian and high-frequency noise but are inherently limited in addressing non-Gaussian and impulsive noise. This highlights the importance of selecting preprocessing strategies based on sensor-specific characteristics and reinforces the role of signal-level processing as a critical foundation for reliable state estimation. From a broader perspective, the results provide practical insights into the design of preprocessing pipelines for quadruped robotics and contribute to improving the robustness of downstream estimation frameworks such as EKF and InEKF. By enhancing measurement consistency, preprocessing can support more stable and accurate state estimation.

However, this study is limited to signal-level analysis and does not include direct evaluation within a complete state estimation framework. In addition, the preprocessing methods are restricted to linear filtering techniques, which are insufficient for handling impulsive disturbances. Future work should explore advanced preprocessing approaches, such as nonlinear or robust filtering methods, and investigate their integration with state estimation algorithms under varying locomotion conditions..

Author Contributions: Conceptualization: M.D.N., M.T.N. and H.T.N.; Methodology: M.D.N. and B.T.T.N.; Software: L.D.Q. and D.T.N.; Validation: M.T.N., T.C.V. and D.M.N.; Formal analysis: H.T.N.; Investigation: M.T.N.; Resources: D.M.N.; Data curation: L.D.Q. and D.T.N.; Writing—original draft preparation: M.T.N., T.C.V. and D.M.N.; Writing—review and editing: M.T.N.; Visualization: M.D.N.; Supervision: M.T.N.; Project administration: M.T.N.; Funding acquisition: M.D.N. All authors have read and agreed to the published version of the manuscript.

Funding: This research received no external funding.

Data Availability Statement: Data can be provided upon request.

Acknowledgments: The authors would like to thank Thai Nguyen University of Technology (Project T2025-NCS11), Viet Nam.

Conflicts of Interest: The authors declare no conflict of interest.

References

[1] A. Hamrani, M. M. Rayhan, T. Mackenson, D. McDaniel, and L. Lagos, "Smart quadruped robotics: a systematic review of design, control, sensing and perception," *Adv. Robot.*, vol. 39, no. 1, pp. 3–29, Jan. 2025, doi: 10.1080/01691864.2024.2411684.

[2] Y. Fan, Z. Pei, C. Wang, M. Li, Z. Tang, and Q. Liu, "A Review of Quadruped Robots: Structure, Control, and Autonomous Motion," *Adv. Intell. Syst.*, vol. 6, no. 6, Jun. 2024, doi: 10.1002/aisy.202300783.

[3] C. D. Bellicoso *et al.*, "Advances in real-world applications for legged robots," *J. F. Robot.*, vol. 35, no. 8, pp. 1311–1326, Dec. 2018, doi: 10.1002/rob.21839.

[4] A. Majithia *et al.*, "Design, motions, capabilities, and applications of quadruped robots: a comprehensive review," *Front. Mech. Eng.*, vol. 10, Aug. 2024, doi: 10.3389/fmech.2024.1448681.

[5] M. V. Minniti, R. Grandia, F. Farshidian, and M. Hutter, "Adaptive CLF-MPC With Application to Quadrupedal Robots," *IEEE Robot. Autom. Lett.*, vol. 7, no. 1, pp. 565–572, Jan. 2022, doi: 10.1109/LRA.2021.3128697.

[6] W. Li, Y. Liao, X. Xiong, C. Li, and Y. Lou, "Hybrid Real-Time State Estimation for Quadruped Robots With Proprioceptive Sensors," *IEEE Trans. Ind. Electron.*, vol. 73, no. 2, pp. 2656–2667, Feb. 2026, doi: 10.1109/TIE.2025.3607996.

[7] P. Ghorai, A. Eskandarian, Y.-K. Kim, and G. Mehr, "State Estimation and Motion Prediction of Vehicles and Vulnerable Road Users for Cooperative Autonomous Driving: A Survey," *IEEE Trans. Intell. Transp. Syst.*, vol. 23, no. 10, pp. 16983–17002, Oct. 2022, doi: 10.1109/TITS.2022.3160932.

[8] H. Belaidi and F. Demim, "NURBs Based Multi-robots Path Planning with Obstacle Avoidance," *J. Comput. Theor. Appl.*, vol. 1, no. 4, pp. 478–491, May 2024, doi: 10.62411/jcta.10387.

[9] T.-Y. Lin, T. Li, W. Tong, and M. Ghaffari, "Proprioceptive Invariant Robot State Estimation," *arXiv*. Feb. 20, 2024. doi: 10.48550/arXiv.

[10] G. Fink and C. Semini, "Proprioceptive Sensor Fusion for Quadruped Robot State Estimation," in *2020 IEEE/RSJ International Conference on Intelligent Robots and Systems (IROS)*, Oct. 2020, pp. 10914–10920. doi: 10.1109/IROS45743.2020.9341521.

[11] M. Camurri *et al.*, "Probabilistic Contact Estimation and Impact Detection for State Estimation of Quadruped Robots," *IEEE Robot. Autom. Lett.*, vol. 2, no. 2, pp. 1023–1030, Apr. 2017, doi: 10.1109/LRA.2017.2652491.

[12] R. Hartley, M. G. Jadidi, L. Gan, J.-K. Huang, J. W. Grizzle, and R. M. Eustice, "Hybrid Contact Preintegration for Visual-Inertial-Contact State Estimation Using Factor Graphs," in *2018 IEEE/RSJ International Conference on Intelligent Robots and Systems (IROS)*, Oct. 2018, pp. 3783–3790. doi: 10.1109/IROS.2018.8593801.

[13] T.-Y. Lin, R. Zhang, J. Yu, and M. Ghaffari, "Legged Robot State Estimation using Invariant Kalman Filtering and Learned Contact Events," *arXiv*. Nov. 29, 2021. [Online]. Available: http://arxiv.org/abs/2106.15713

[14] Y. Nisticò, J. C. V. Soares, L. Amatucci, G. Fink, and C. Semini, "MUSE: A Real-Time Multi-Sensor State Estimator for Quadruped Robots," *IEEE Robot. Autom. Lett.*, vol. 10, no. 5, pp. 4620–4627, May 2025, doi: 10.1109/LRA.2025.3553047.

[15] L. Q. Dinh, D. T. Nguyen, T. C. Vu, T. V. Nguyen, and M. T. Nguyen, "Comprehensive Review of Security Problems in Mobile Robotic Assistant Systems: Issues, Solutions, and Challenges," *J. Comput. Theor. Appl.*, vol. 2, no. 2, pp. 182–201, Sep. 2024, doi: 10.62411/jcta.11408.

[16] S. Dasgupta, D. Das, M. Hoque, and I. Bhattacharya, "An Intelligent Route Planning Approach Using Modified Particle Swarm Optimization for Robot Assisted Minimally Invasive Surgery," *J. Comput. Theor. Appl.*, vol. 2, no. 4, pp. 498–510, Apr. 2025, doi: 10.62411/jcta.12473.

[17] C. Pan, R. Hao, J. Yu, and L. Zhang, "Pose Estimation Algorithm for Quadruped Robots Based on Multi-Sensor Fusion," in *2024 International Symposium on Intelligent Robotics and Systems (ISoIRS)*, Jun. 2024, pp. 1–11. doi: 10.1109/ISoIRS63136.2024.00009.

[18] J. He and F. Gao, "Mechanism, Actuation, Perception, and Control of Highly Dynamic Multilegged Robots: A Review," *Chinese J. Mech. Eng.*, vol. 33, no. 1, p. 79, Dec. 2020, doi: 10.1186/s10033-020-00485-9.

[19] L. Wijayarathne, Z. Zhou, Y. Zhao, and F. L. Hammond, "Real-Time Deformable-Contact-Aware Model Predictive Control for Force-Modulated Manipulation," *IEEE Trans. Robot.*, vol. 39, no. 5, pp. 3549–3566, Oct. 2023, doi: 10.1109/TRO.2023.3286070.

[20] G. Soter, A. Conn, H. Hauser, and J. Rossiter, "Bodily Aware Soft Robots: Integration of Proprioceptive and Exteroceptive Sensors," in *2018 IEEE International Conference on Robotics and Automation (ICRA)*, May 2018, pp. 2448–2453. doi: 10.1109/ICRA.2018.8463169.

[21] J. Kelly and G. S. Sukhatme, "A General Framework for Temporal Calibration of Multiple Proprioceptive and Exteroceptive Sensors," 2014, pp. 195–209. doi: 10.1007/978-3-642-28572-1_14.

[22] S. Li *et al.*, "Feature-Triggered Short-Term Drift Calibration of IMU Position on Human Lower Limbs Under Random Motions With Convolution–Deconvolution Prediction Models," *IEEE Sens. J.*, vol. 25, no. 23, pp. 43487–43499, Dec. 2025, doi: 10.1109/JSEN.2025.3621264.

[23] M. D. Nguyen *et al.*, "Fusion of Wheel Encoded Data and RFID Signals using Kalman Filter for Robot Indoor Localization," *J. Futur. Artif. Intell. Technol.*, vol. 2, no. 3, pp. 328–342, Jul. 2025, doi: 10.62411/faith.3048-3719-126.

[24] M. Wan, D. Liu, J. Wu, L. Li, Z. Peng, and Z. Liu, "State Estimation for Quadruped Robots on Non-Stationary Terrain via Invariant Extended Kalman Filter and Disturbance Observer," *Sensors*, vol. 24, no. 22, p. 7290, Nov. 2024, doi: 10.3390/s24227290.

[25] S. Yang, Q. Yang, R. Zhu, Z. Zhang, C. Li, and H. Liu, "State estimation of hydraulic quadruped robots using invariant-EKF and kinematics with neural networks," *Neural Comput. Appl.*, vol. 36, no. 5, pp. 2231–2244, Feb. 2024, doi: 10.1007/s00521-023-08755-y.
[26] J. Sun, L. Zhou, B. Geng, Y. Zhang, and Y. Li, "Leg State Estimation for Quadruped Robot by Using Probabilistic Model With Proprioceptive Feedback," *IEEE/ASME Trans. Mechatronics*, vol. 30, no. 3, pp. 1876–1887, Jun. 2025, doi: 10.1109/TMECH.2024.3421251.
[27] K.-C. Han and J.-Y. Kim, "Posture stabilizing control of quadruped robot based on cart-inverted pendulum model," *Intell. Serv. Robot.*, vol. 16, no. 5, pp. 521–536, Nov. 2023, doi: 10.1007/s11370-023-00480-8.
[28] G. Fink, "Proprioceptive Sensor Dataset for Quadruped Robots," *IEEE Dataport*. IEEE Dataport, 2019. doi: 10.21227/4vxz-xw05.